

MODELLING POINT CLOUDS FOR PRECISE STRUCTURAL DEFORMATION MEASUREMENT

S. J. Gordon*, D. D. Lichti, M. P. Stewart and J. Franke

Western Australian Centre for Geodesy, Curtin University of Technology
GPO Box U1987, Perth, WA, 6845, Australia
S.Gordon@curtin.edu.au

KEY WORDS: Laser scanning, Metrology, Modelling, Monitoring, Point Cloud, TLS

ABSTRACT:

Terrestrial laser scanners can rapidly acquire thousands of 3D points over a structure. The individual scan points are of relatively low precision ($\pm 2\text{mm}$ – $\pm 50\text{mm}$) depending on the instrument type. However, combining the dense 3D point data with judicious modelling strategies can produce a very precise surface model. A surface model has advantages for structural deformation monitoring where deflections are small ($< 50\text{mm}$) and the shape change can potentially vary across the entire structure. The notion of the research presented in this paper is to exploit the dense 3D point data (clouds) to assess the sensitivity of laser scanners for measuring structural deformation. Two experiments have been undertaken where, in each experiment, a beam was subjected to controlled loading. The first experiment involved a timber beam (5.0m x 0.2m x 0.1m) mounted on an indoor load-testing frame. The beam was subject to a maximum of 40mm of vertical deflection. The focus of the second experiment was a concrete beam (7.0m x 0.5m x 0.5m) placed on an outdoor load-testing frame where it was loaded until failure. All loading was induced by a hydraulic jack and occurred in increments permitting measurements to be made by laser scanners. A Riegl LMS-Z210 laser scanner was used for both experiments and a Cyra Cyra 2500 was available for the first. The scanner measurements were validated using close-range photogrammetry (accuracy of 1:40,000 of object size or better).

1. INTRODUCTION

The difficulty of monitoring deflections is finding a spatial measurement technique that encompasses numerous desirable properties, such as reliability, accuracy, low-cost and ease of installation (Stanton et al., 2003). There are many methods that purport some of these advantages but not all. For example, digital photogrammetry can be relatively inexpensive and highly precise; as well as offering rapid, remote, three-dimensional data capture and images which provide a permanent visual record of the test. However, the necessary use of targets may be disadvantageous in some circumstances, especially when the object is hazardous to operators or inaccessible. Furthermore, unless convergent imaging is practiced, the depth dimension can be poorly observed. This can occur when the laboratory lacks sufficient space to satisfy an even geometric distribution of exposure stations. The photogrammetric process also lacks scale definition, requiring measurements to be acquired using additional instrumentation, such as a precise scale bar.

Traditionally, contact sensors, such as dial gauges and linear-variable-differential transducers (LVDTs), are employed for structural deflection experiments because of their high precision spatial measurement capabilities. However, their contact nature precludes them from use during the final stages of destructive load testing and they are only capable of acquiring measurements in one dimension. Importantly, the number of monitoring sites, or data density, is limited by the number of contact sensors available for the experiment. This is also true for target availability in photogrammetric metrology, although it is less of a problem since photogrammetric targets are inexpensive and may be quickly placed on the object of interest and its stable surrounds.

Terrestrial laser scanners (TLSs) are modern geomatic data capture instruments that offer numerous measurement benefits including three-dimensional data capture, remote and non-contact (i.e. targetless) operation, a permanent visual record and dense data acquisition. TLSs are currently being used in a variety of projects, including heritage mapping, as-built documentation and topographic surveys. However, the precision of TLSs is not perceived adequate for industrial metrology applications, such as deformation monitoring.

The advantage of TLSs is that, although individual sample points are low in precision (e.g. $\pm 2\text{mm}$ to $\pm 50\text{mm}$), modelling of the entire point cloud may be effective for explaining the change of shape of a structure. A modelled surface will be a more precise representation of the object than the unmodelled observations. In light of this notion, a methodology for measuring structural deformation, relying on theoretical aspects of beam mechanics and implemented by constrained least-squares curve fitting, has been developed and is presented in Section 2. A statistical test for assessing the redundancy of estimated parameters is given in Section 3. The results of two structural deformation monitoring experiments, involving beams (one concrete and one timber) being loaded in a load-testing frame, used to test the analytical modelling strategy are presented in Sections 4 and 5. Both experiments were controlled with convergent digital photogrammetry. A discussion focussing on instrument set up is given in Section 6 and the conclusions are presented in Section 7.

* Corresponding author.

2. BEAM DEFLECTION BY INTEGRATION

There are numerous 3D data modelling techniques available, such as creating a TIN or gridding. Selection of an appropriate surface model is critical to permit the accurate computation of an object's deformation. The method chosen to model vertical deflections in these experiments is based on forming analytical models representing the physical bending of the beam. The models are derived from first principles of beam deflection by integration, which essentially yields low order polynomials (no higher than a cubic in the experiments presented later). Once these models are developed, the coefficients of the polynomials are solved as unknown parameters in a least-squares estimation process. The observations consist of the several hundred 3D point samples from each TLS. A single functional model is used to represent the beam deflection but the parameters of the model are estimated for each deflection epoch.

A beam which is subjected to loading will bend into an arc which can be defined by a curvature function (Beer and Johnston, 1992). The equation, known as the governing differential equation for the elastic curve, is shown in Eq. 1. It is a second-order linear differential equation and is composed of the beam's bending moment, M , which is a function of x , the distance along the beam, divided by the modulus of elasticity, E , and moment of inertia, I . The bending moment is a reaction to an applied force which causes a structure to rotate or bend. This equation holds true for small deflections. Integrating Eq. 1 twice, with respect to x , will yield the function of deflection. This function will permit the vertical deflections to be computed. A more detailed explanation of beam deflection by integration may be sought in Beer and Johnston (1992).

$$\frac{\partial^2 z}{\partial x^2} = \frac{M(x)}{EI} \quad (1)$$

The modelling process can be demonstrated using an example. Consider a simply supported beam (i.e. a support point at each of its ends) consisting of a load point, P , at the centre of the beam, located at x_p . A sketch is shown in Figure 1.

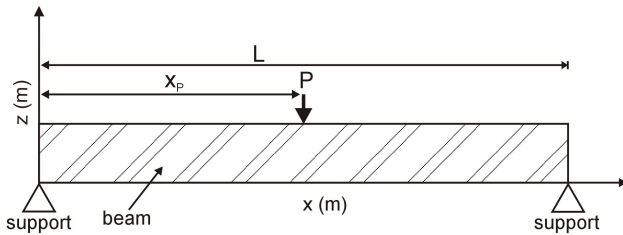


Figure 1. Schematic diagram for the timber beam.

The bending moment, represented by two functions (one each side of x_p), is linear, maximum at x_p and zero at each support point. Two successive integrations yield a cubic equation. The generalised form of the compound cubic polynomial is given in Eq. 2 and may be adopted for curve fitting the beam shown in Figure 1. An additional term in the y -axis direction is added to model any linear tilts about the x -axis (ω rotation) that may be evident in the 3D scan cloud of the beam. Justification for this term is given later. A detailed derivation of the model (and curve fitting constraints) can be found in Gordon et al. (2003a).

$$z = \begin{cases} z_1 = a_{30}x^3 + a_{10}x + a_{00} + a_{01}y & ; 0 \leq x \leq x_p \\ z_2 = b_{30}x^3 + b_{20}x^2 + b_{10}x + b_{00} + a_{01}y & ; x_p \leq x \leq L \end{cases} \quad (2)$$

3. STATISTICAL TESTING OF ESTIMATED PARAMETERS

The modelling process yields low-order polynomials that are naturally prone to high parameter correlation, which indicate that the functional model is not efficient in modelling the curvature. A test is adopted to assess the significance of the estimated parameters for each of the solutions. Parameters that are found to be statistically insignificant should be removed using an appropriate elimination strategy, such as backward stepwise selection, to alleviate high coupling. Statistical testing of parameters is routinely performed to ensure that estimated models are optimised for the task at hand. Examples in the geomatics industry may be found in photogrammetry, such as identification of insignificant additional parameters in aerial photogrammetry (Jacobsen, 1982). Zhong (1997) shows that polynomials, used for the interpolation of GPS geoid heights, can be statistically tested. The author's recommendations include a methodology for optimal parameter selection for polynomial models.

3.1 Global Significance Test

The first step in the statistical testing process involves analysing the overall model for the significance of its parameters. Following the methodology recommended by Zhong (1997), the F-test is adopted and a global test statistic, F , is computed using:

$$F = \frac{\hat{\mathbf{x}}^T \mathbf{C}_{\hat{\mathbf{x}}}^{-1} \hat{\mathbf{x}}}{t \hat{\sigma}_0^2} \sim \tilde{F}_{1,r} \quad (3)$$

where $\mathbf{C}_{\hat{\mathbf{x}}}$ is the covariance matrix of estimated parameters, $\hat{\sigma}_0^2$ is the estimated variance factor, r is the degrees of freedom, t is the number of parameters in $\hat{\mathbf{x}}$, the parameter vector and \tilde{F} is Fisher's distribution. Since the least-squares estimation process involves hundreds of point samples, the degree of freedom is always very high compared to small number of unknown parameters, assuming that the observations are uncorrelated.

3.2 Individual Parameter Significance Test

It is possible to extend the analysis to the testing of each individual parameter using (Zhong, 1997):

$$F_i = \frac{\hat{x}_i^2}{\hat{\sigma}_0^2 \sigma_{\hat{x}_i}^2} \sim \tilde{F}_{1,r} \quad (4)$$

where \hat{x}_i^2 is the square of the i^{th} estimated parameter, $\sigma_{\hat{x}_i}^2$ is the variance for that estimated parameter, $\hat{\sigma}_0^2$ is the estimated variance factor and F_i is the individual parameter test statistic.

4. EXPERIMENT I: TIMBER BEAM

The beam modelling strategy and parameter testing procedure was assessed using two laboratory-based experiments. The first experiment involved the controlled loading of a timber beam on an indoor test frame based in the Department of Civil Engineering laboratories at Curtin University. The beam, which had dimensions of 5.2m x 0.2m x 0.1m, was supported at each of its ends. The loading was applied by a hydraulic jack that was positioned at the centre of the beam.

A total of eight load increments were applied whereby a nominal 5mm of vertical displacement (at the centre of the beam) was induced on each occasion. A 'dead load' was collected at the beginning of the testing permitting the capture of a zero-load case. A dial gauge was positioned in the approximate centre of the beam and was used by the jack operator to assist in determining each 5mm increment (it was not used for analysis). The total downward vertical deflection measured at the centre of the beam was approximately 40mm.

4.1 Instrumentation

Two TLSs were used during these experiments: a Cyra Cyrax 2500 (Leica Geosystems, 2004) and a Riegl LMS-Z210 (Riegl, 2004). The Cyrax 2500 is capable of acquiring three-dimensional points at a rate of 1000Hz. The scanner's range precision is $\pm 4\text{mm}$ (1σ) and it possesses a coordinate precision of $\pm 6\text{mm}$ (1σ). The LMS-Z210 collects points at a rate of 6000Hz. Though faster than the Cyrax 2500, its range precision of $\pm 25\text{mm}$ (1σ) is much poorer. Its point coordinate precision, at the distances used in this research ($<10\text{m}$), is commensurate with its range precision (i.e. $\pm 25\text{mm}$).

With respect to imaging resolution, the Cyrax 2500 has a minimum sampling interval of less than 1mm (at 10m) but this resolution is tempered somewhat by a laser beamwidth of approximately 6mm at the same range (Lichti, 2004). The LMS-Z210 has a relatively large beamwidth compared to most commercially available TLSs. The beamwidth is approximately 30mm at 10m and the TLS has a minimum sampling interval of 13mm at 10m. Further information regarding these instruments may be sought from the respective manufacturer's website.

Close-range photogrammetry was used to control both major experiments. A Kodak DC420 with a CCD array of 1524 by 1012 pixels (square pixels with a $9\mu\text{m}$ width) fitted with a 14mm lens was used. In all cases, the focal ring was set to infinity and secured with tape. The cameras were calibrated before and after each experiment.

4.2 Data Collection

The Cyrax 2500 was located 5.4m from the centre of the timber beam and to the left of the laboratory and the LMS-Z210 was positioned 6.4m from the centre of the beam away to the right of the laboratory. Both instruments were set up on stable footings and were not moved for the entire experiment. It was assumed that the TLSs were completely stationary for the duration of the testing, which lasted two hours. Neither instrument was force-centred over a pre-marked known point. The LMS-Z210 was levelled but the Cyrax 2500 was not (it does not have a level bubble).

During loading, high-resolution scans were collected at each epoch by each of the scanners. The Cyrax 2500, which has a relatively slower data capture rate than the LMS-Z210, only acquired a single scan per load epoch. The LMS-Z210, which offers a relatively coarser coordinate precision than the Cyrax 2500, captured three repeat scans of the beam that were averaged to produce a single mean scan, theoretically reducing the coordinate standard deviation of points to $\pm 14\text{mm}$.

Twenty-five photogrammetric targets were affixed to the face of the beam. Others were placed around the room and on stable components of the test frame. The photogrammetric coordination of the array of targets provided a common coordinate system for the TLS datasets.

4.3 Photogrammetric Results

Photogrammetric data processing task was performed using *Australis* digital photogrammetric software (Fraser and Edmundson, 2000). The photogrammetric network was treated as a free network adjustment and the datum was defined by the stable targets. Several scale measurements were made using a steel band. The RMS of coordinate standard deviations of the targets was $\pm 0.14\text{mm}$ (1σ) and $\pm 0.15\text{mm}$ (1σ) for X and Y, respectively and $\pm 0.04\text{mm}$ (1σ) for Z, the most crucial direction for this experiment.

4.4 Scan Data Pre-Processing

Since both TLSs were set up at different positions, both scanners used the targets coordinated by the photogrammetric process to resect their relative positions and orientations. The dead load case for each TLS was used for this purpose. Once the resection parameters were derived, subsequent clouds were transformed into the photogrammetric coordinate system. A total of 11 control points were used for the Cyrax 2500 resection and 15 control points were used for the LMS-Z210 resection. Whilst the transformation process serves as an additional error source (Gordon and Lichti, 2004), it was a necessary task to enable direct comparisons of vertical deflections from the photogrammetric and TLS data sources.

Once all scan data were in the same reference frame, the individual scan clouds were manually edited to remove all scan points except for those on the top surface of the beam. The top of the beam was used for analysis because vertical deflection was the most pertinent for subsequent structural analyses. The extracted beam top clouds, though composed of irregularly spaced points, had an approximate sample interval of 5mm for the Cyrax 2500 and 15mm – 20mm for the LMS-Z210.

4.5 Beam Modelling

The timber beam conforms to the simply supported example shown in Figure 1. Therefore, Eq. 2 was adopted for this experiment. All TLS data for a single epoch were processed in one adjustment, thus simultaneously solving for the left (z_1) and right (z_2) models. The mean number of points used for each solution was 7364 for the Cyrax 2500 and 1099 for the LMS-Z210. Clearly, there were more observations available for the Cyrax 2500 dataset, which was a function of the smaller sampling interval offered by that TLS. The overall RMS of residuals from the least-squares adjustments was $\pm 0.6\text{mm}$ for the Cyrax 2500 and $\pm 5.4\text{mm}$ for the LMS-Z210. The difference in the size of residuals largely reflects the observational precision of each scanner.

4.6 Statistical Testing of Estimated Parameters

Statistical testing was performed on each solution. The smallest critical value computed for the global test was $F(0.01;8,876) = 2.60$ (occurring for load 2 for the LMS-Z210) at a level of significance of 1%. The smallest computed test statistic (Eq. 3) was 185.9 for the LMS-Z210 during load case 6. All models satisfied their respective critical values. Therefore, no parameter removal was necessary given these statistical test results.

The test was extended to individual parameter testing. The smallest of all critical values used for comparison was 6.80. The smallest computed test statistic (Eq. 4) was 20.2 (parameter b_{30} from the dead load epoch for the LMS-Z210). Analysis of the results revealed that each parameter statistic grew larger as testing went on. As the beam experiences increasing amounts of deflection, the individual parameters are required to model the additional curvature that, in turn, increases their significance in the model. In all cases, the intercept terms (a_{00} and b_{00}) exhibited much greater influence in the models than any other parameter. None of the estimated parameters were deemed insignificant at the 1% significance level for any of the models and no parameter elimination is required using this test. The developed models are therefore considered appropriate. The statistical testing supplies confidence towards the derivation of the models since they were developed from first principles of beam deflection by integration and that each parameter theoretically has a sound physical basis for inclusion in the model.

4.7 Vertical Deflections

Vertical deflections were derived using the estimated models for each of the eight load epochs. The x and y coordinates of each of the 13 photogrammetric targets (constituting the top row of targets on the beam) were passed into the estimated models to compute a z -coordinate. Only the top row of targets was used because they were the closest to the beam top. The z -coordinates were then used to determine vertical deflections between epochs. Each TLS set of vertical deflections (i.e. for the Cyrax 2500 and the LMS-Z210) was compared to the vertical deflections produced by the photogrammetry and the differences are shown in Table 1.

Nominal Vertical Deflection (mm)	RMS of Differences (mm)	
	Cyrax 2500	LMS-Z210
5	± 0.12	± 3.6
10	± 0.14	± 4.1
15	± 0.47	± 3.2
20	± 0.26	± 2.3
25	± 0.24	± 5.0
30	± 0.27	± 5.0
35	± 0.30	± 2.7
40	± 0.34	± 1.4
Total RMS	± 0.29	± 3.6

Table 1. RMS of differences between TLS-derived and photogrammetry-derived vertical deflections using 13 targets per deflection case.

Table 1 indicates that the estimated models using Cyrax 2500 data, compared to the benchmark photogrammetry, give an overall RMS of differences of ± 0.29 mm. The largest RMS of differences is ± 0.47 mm for the 15mm deflection case. The

overall RMS of differences for the LMS-Z210 is ± 3.6 mm. The maximum RMS is ± 5.0 mm for the 25mm deflection case. The overall RMS values represent a factor of improvement (in precision) of 21 times for the Cyrax 2500 and 7 times for the LMS-Z210 over the coordinate precision of each TLS.

The linear term, a_{01} , was used to model rotation about the x -axis. In adjustments undertaken without the y -term, plots of residuals versus y -axis coordinates for the Cyrax 2500 shows a distinct tilt of approximately 1.7° and a tilt of 2.7° for the LMS-Z210 indicating that the beam top was not horizontal in the reference coordinate system for all cases. Analysis of the a_{01} parameter shows that it was consistently the same size for the Cyrax 2500 dataset (-0.030 ± 0.001) but fluctuated in the LMS-Z210 results (-0.047 ± 0.017). This was primarily due to the sparsity of data in the y -direction of the LMS-Z210 compared to the Cyrax 2500. The uncertainty in the determination of the a_{01} parameter caused vertical deflection measurements to be worse for the LMS-Z210 when compared to results where y -term was omitted (overall RMS of differences ± 2.1 mm for all cases where the y -term was omitted). Cyrax 2500 results were better with the y -term included and were worse without it (overall RMS of differences ± 0.46 mm without the y -term).

5. EXPERIMENT II: CONCRETE BEAM

The second major experiment conducted to test the analytical modelling strategy involved an ‘L-shaped’ (in cross section) 7.2m x 0.5m x 0.5m reinforced concrete beam that was loaded until failure. The beam was formerly part of an old bridge, which had been dismantled for the purpose of controlled laboratory testing. The beam was placed in a heavy-duty outdoor testing frame and supported at each end. The two load points were near the centre of the beam.

The beam was loaded in increments up to 240kN (approximately 13mm of vertical deflection), at which point the load was relaxed (epoch seven). This permitted the zero-datum of the contact sensors to be redefined. Loading resumed and continued in increments until the beam failed (490kN). The purpose of this loading schedule was to ascertain the elastic properties of the concrete beam.

5.1 Set Up and Targeting

An LMS-Z210 was situated 7m from the beam and directly in front of the test frame (see Figure 2). It was set up as high as possible on the tripod enabling acquisition of points from the top surface of the beam. Similar to the first experiment, the position and orientation of the TLS was determined by resection. Photogrammetry was used to benchmark the experiment and the photogrammetric coordinate system provided the reference frame for the experiment.

5.2 Data Collection

A total of 13 measurement epochs were acquired during the period of testing. A dead load epoch was acquired at epoch zero and also at epoch seven (where the load on the beam was relaxed). The final measurement epoch where the beam was intact was epoch 12 but contact sensors were removed prior to this (after recording epoch 10) because failure was imminent. The impending specimen failure did not affect the remote measurement techniques (i.e. photogrammetry and TLS) highlighting, through practice, the advantage of a remote

measurement technique. At each epoch, three repeat scans were collected and averaged to produce one mean scan.



Figure 2. Concrete beam and the Riegl LMS-Z210.

5.3 Photogrammetric Results

Each photogrammetric epoch consisted of nine images from around the front of the beam ensuring strong convergent imaging angles. Photogrammetric adjustment was undertaken in a similar fashion to the timber beam experiment. The stable targets were used to define the datum in a free-network adjustment. Several scale measurements were acquired using a steel band. The RMS of the estimated coordinate precision of the photogrammetric targets was $\pm 0.12\text{mm}$ (1σ), $\pm 0.21\text{mm}$ (1σ) and $\pm 0.09\text{mm}$ (1σ) for X, Y and Z respectively.

5.4 Derivation and Adoption of Beam Deflection Models

Unlike the timber beam, the two load points used for the concrete beam experiment meant that it was divided into three sections. Figure 3 is a schematic diagram of the concrete beam.

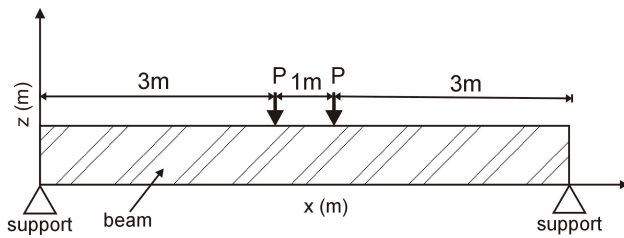


Figure 3. Schematic diagram for the concrete beam

The load points were situated 3m and 4m in from the left of the beam. Eq. 5 is the model adopted for the concrete beam. A y-term was included to cater for rotations about the x-axis in the concrete beam. Results indicated that the beam carried approximately 1.5° of rotation compared to the horizontal plane of the reference frame.

$$z(x) \begin{cases} z_1(x) = a_{30}x^3 + a_{10}x + a_{00} + a_{01}y & ; 0 \leq x \leq 3 \\ z_2(x) = b_{20}x^2 + b_{10}x + b_{00} + a_{01}y & ; 3 \leq x \leq 4 \\ z_3(x) = c_{30}x^3 + c_{20}x^2 + c_{10}x + c_{00} + a_{01}y & ; 4 \leq x \leq 7 \end{cases} \quad (5)$$

5.5 Analysis of the Adjustment

The overall RMS of residuals was $\pm 2.5\text{mm}$ for the least-squares estimation using a mean of 268 points. This is two times better than the fit of the timber beam models using the LMS-Z210 and most likely due to the extra terms of the concrete beam deflection functions making it more flexible when modelling the data. The mean value estimated for the y-term from all 12 load epochs was 0.027 ± 0.006 (unitless). The beam top tilt, revealing itself as the gradient of the y-term, was more precisely determined than in the timber beam experiment.

5.6 Statistical Testing of Estimated Parameters

The smallest critical value for all global tests was $F(0.01; 11, 188) = 2.39$. The smallest computed global test statistic (Eq. 3) is much greater than the critical value for all cases suggesting that the models are adequate. However, there are six instances where the individual test statistics for the c_{30} parameter are less than their respective critical value at a 1% significance level. There is also one instance where the test statistic for the a_{10} term is less than its critical value (load case 6). For instances where the test statistic is less than the critical value, the parameter does not have significant influence on the model and it should be removed. Consequently, where required, each model was revised and recomputed until all parameters satisfied the individual parameter statistical test.

5.7 Vertical Deflections

Computation of vertical deflections was undertaken in a similar fashion to the timber beam experiment. Planimetric coordinates of 12 photogrammetric targets were passed through the estimated models producing a height coordinate. The number of targets varied depending on their visibility in the photogrammetric images. Vertical deflections were computed by differencing the height coordinates. Table 2 shows the original differences for the entire 11-parameter model (Eq. 5). The table also includes the RMS of differences for the revised models and shows which parameters were eliminated.

The total RMS of differences has not changed despite using models that have had terms removed. Load cases 6 and 10 have actually (marginally) improved in accuracy. Load cases 1, 4, 9 and 11 are equivalent, or slightly worse, in accuracy compared to the original 11-parameter model.

6. DISCUSSION

It is unknown why the LMS-Z210 performed slightly better for the second experiment (concrete beam). The imaging geometry was similar in both instances whereby the TLS was 6.4m from the (front, centre) of the timber beam with a zenith angle of approximately $96^\circ 40'$ and 7m from the front, centre of the concrete beam with a zenith angle of approximately $96^\circ 17'$. The only difference was that the concrete beam was outdoors and the TLS was not set in front of the timber beam but offset to one side. The mean size of the point clouds (of the beam tops) were actually smaller for the concrete beam (mean of 268 points) compared to the timber beam (mean of 1099 points) implying that the sample size was not the reason.

Epoch	Maximum vertical deflection (mm)	Number of Targets	11 parameter RMS (mm)	Revised model RMS (mm)	Eliminated parameters
1	2.1	12	±1.1	±1.3	c ₃₀
2	4.1	12	±0.9	±0.9	
3	6.0	12	±3.7	±3.7	
4	8.0	12	±1.7	±1.7	c ₃₀
5	10.0	12	±2.4	±2.4	
6	12.9	12	±2.3	±2.1	c ₃₀ , a ₁₀
7	0.9	11	±2.1	±2.1	
8	4.1	12	±1.2	±1.2	
9	8.3	12	±2.0	±2.1	c ₃₀
10	13.2	11	±3.2	±2.8	c ₃₀ , a ₁₀
11	28.8	12	±2.7	±2.8	c ₃₀
12	48.3	11	±3.3	±3.5	
	Total	RMS	±2.4	±2.4	

Table 2. Differences of vertical deflections between the LMS-Z210 and photogrammetry.

Most of the commercially available TLSs have a sufficiently large vertical field of view permitting them to be positioned high above the test structure or whatever the case may be. Potentially, the TLS *does not* need to be levelled. Measurements would be benefited by tilting the TLS towards the structure. The critical factor is to maintain a stable placement so that the TLS remains stationary for the duration of testing. Despite the necessity of a thoughtful set up, both experiments showed that it was still possible to successfully measure deformation even though the imaging geometry was suboptimal and scan data were scarce.

7. CONCLUSIONS

An analytical modelling approach was developed to detect and measure vertical deformation. It involved representing the beam with a compound polynomial containing parameters that have a sound physical origin derived from first principles of beam deflection mechanics. The solutions were found to suffer from high parameter correlations.

Statistical testing of the significance of the estimated parameters in the polynomial models proved an effective method of removing insignificant parameters. All timber beam solutions passed the F-tests. Testing of the parameters in the concrete beam example revealed parameters that were not a significant influence in the model. A revised model was created for those cases and was compared to the photogrammetric benchmark data. It was shown that the statistical testing of parameters could be successfully used to remove redundant parameters without compromising the accuracy of the model. These tests were conducted, however, in relatively controlled conditions.

This modelling avoids the arbitrary nature inherent in some other methods, such as gridding (Gordon et al., 2003b). The sub-millimetre results for the Cyra Cyrax 2500 place it in the same accuracy league as close-range photogrammetry (at least, for non-metric cameras). The perceived main advantage of photogrammetry over TLS is its high precision. The additional advantages of TLS, however, include full surface representation

(as opposed to a few targets) and also a single set up geometry that does not have an inherently weak dimension (as photogrammetry has in depth). Furthermore, the reflectorless nature of TLS does not require targets except for validation.

8. REFERENCES

- Beer, F.P. and Johnston, E.R., 1992. *Mechanics of Materials*. McGraw-Hill Book Company, Berkshire, England, 738 pages.
- Fraser, C.S. and Edmundson, K.L., 2000. Design and Implementation of a Computational Processing System for Off-Line Digital Close-Range Photogrammetry. *ISPRS Journal of Photogrammetry and Remote Sensing*, 55(2), pp. 94 - 104.
- Gordon, S.J. and Lichti, D.D., 2004. Terrestrial Laser Scanners with a Narrow Field of View: The Effect on 3D Resection Solutions. *Survey Review*, 37(292), In press.
- Gordon, S.J., Lichti, D.D., Chandler, I., Stewart, M.P. and Franke, J., 2003a. Precision Measurement of Structural Deformation using Terrestrial Laser Scanners. In: *Optical 3D Methods*, Zurich, Switzerland, 22 - 25 September, 8 pages.
- Gordon, S.J., Lichti, D.D. and Stewart, M.P., 2003b. Structural Deformation Measurement using Terrestrial Laser Scanners. In: *11th International FIG Symposium on Deformation Measurements*, Santorini Island, Greece, 25 - 28 May, 8 pages.
- Jacobsen, K., 1982. Attempt at Obtaining the Best Possible Accuracy in Bundle Block Adjustments. *Photogrammetria*, 37(6), pp. 219 - 235.
- Leica Geosystems, 2004. HDS2500 Specifications. http://www.cyra.com/products/hds2500_specs.html (accessed 23 April, 2004).
- Lichti, D.D., 2004. A Resolution Measure for Terrestrial Laser Scanners. In: *ISPRS XX Congress*, Istanbul, Turkey, 12 - 23 July, 6 pages.
- Riegl, 2004. 3D Imaging Sensor LMS-Z210i. http://www.riegl.com/lms-z210i/e_lms-z210i.htm (accessed 23 April, 2004).
- Stanton, J.F., Eberhard, M.O. and Barr, P.J., 2003. A Weight-Stretched-Wire System for Monitoring Deflections. *Engineering Structures*, 25(3), pp. 347 - 357.
- Zhong, D., 1997. Robust Estimation and Optimal Selection of Polynomial Parameters for the Interpolation of GPS Geoid Heights. *Journal of Geodesy*, 71(9), pp. 552 - 561.

9. ACKNOWLEDGEMENTS

The authors wish to thank Dale Keighley and Gerry Nolan from McMullen Nolan and Partners Surveyors Pty. Ltd. (Perth, Australia) for the use of their Cyra Cyrax 2500 and Dr Ian Chandler from the Department of Civil Engineering at Curtin University of Technology, for organising the load tests.